

---

# Time-Resolved Photoresponse in the Resistive Flux-Flow State in Y-Ba-Cu-O Superconducting Microbridges

## Introduction

High-temperature superconductors (HTS's) exhibit many properties that are very desirable for microwave-based telecommunication applications. Their main advantages are low absorption at microwave frequencies<sup>1</sup> and existence of HTS microwave devices based on the controlled vortex flux flow.<sup>2</sup> The most-promising material is the  $\text{YBa}_2\text{Cu}_3\text{O}_{7-x}$  (YBCO) superconductor because of its well-developed technology for the fabrication and patterning of very high quality epitaxial thin films, as well as the ability to produce multilayer microstructures. YBCO is characterized by a very large critical current density  $J_c > 2$  to  $3 \text{ MA/cm}^2$  at nitrogen temperatures<sup>3</sup> and exhibits ultrafast ( $\sim 1$ -ps) voltage photoresponse when optically excited with femtosecond laser pulses.<sup>4</sup> Thus, YBCO thin films and microstructures are good candidates for generating high-power and jitter-free ultrafast electrical transients for ultrawide-frequency-band antennas<sup>5</sup> for mobile communication systems. The ultrawide-band signals can be reflected by any conductor or insulator with dimensions fitting the wavelength of the signal. Therefore, the GHz-bandwidth, jitter-free pulse-driven antennas are desirable devices for high-resolution pulsed-radar systems, operating with a high (GHz) repetition rate of probing signals.

When light is incident on a superconductor, photons with an energy much larger than the superconductor energy gap  $2\Delta$  will break Cooper pairs, resulting in the appearance of highly excited quasiparticles. These excited (hot) carriers thermalize within tens of femtoseconds and, subsequently, relax their excess energy through the electron–phonon interaction process. During the relaxation, the number of excited quasiparticles becomes significantly larger than their equilibrium value, leading to a suppressed  $2\Delta$  value and a nonequilibrium condition in the entire sample. In the space domain, the  $2\Delta$  reduction resulting from the photon absorption generates a so-called “hotspot,” a localized region where superconductivity is highly suppressed or even completely destroyed.<sup>6</sup>

The incoming photons can also generate quantized vortex–antivortex pairs (i.e., oppositely directed fluxons),<sup>7</sup> which can

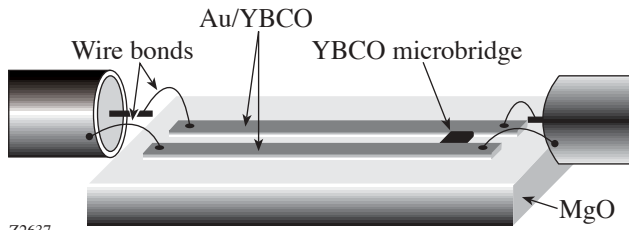
get de-pinned and start moving one toward the other transversely to the direction of the current flow, resulting in a voltage signal. When the temperature inside the optically excited hotspot exceeds the Kosterlitz–Thouless (vortex unbinding) temperature  $T_{KT} \sim E_{vp}/k_B$  (where  $E_{vp}$  is a minimum energy needed to create a vortex–antivortex pair and  $k_B$  is the Boltzmann constant), the vortex–antivortex interaction can get screened, leading to the appearance of essentially unbound single vortices, whose motion brings resistance in the superconducting thin film.<sup>7</sup> At lower temperatures, vortex pairs can be de-pinned by applying a bias current  $I$  that exceeds the critical current  $I_c$ . In this latter case, the superconductor is transferred into a resistive flux state when the Lorentz force exceeds the collective pinning force and bundles of vortices move, leading to a voltage signal across the superconductor.<sup>8</sup>

The aim of this work is to investigate ultrafast voltage transients in optically thick YBCO superconducting microbridges biased with supercritical ( $I > I_c$ ), nanosecond-in-duration current pulses and, simultaneously, excited with femtosecond optical pulses. The above experimental arrangement allowed us to study the superconductor photoresponse in the resistive flux-flow state. The photoresponse voltage transients were recorded, and their amplitude versus bias current, laser fluence, and hotspot area were investigated. The maximal repetition rate of light-triggered YBCO bridges for applications as high-power, jitter-free, electrical pulse generators has been determined. The next section presents the test sample configuration and our experimental setup designed for time-synchronized, simultaneous electrical and optical excitations of YBCO microbridges. The last two sections present our experimental results and the summary and conclusions of our work.

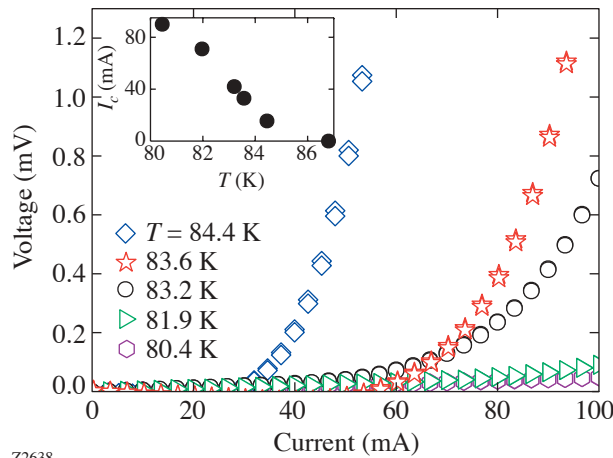
## Sample Design and Experimental Setup

Our experimental samples consisted of  $50\text{-}\mu\text{m}$ -long,  $25\text{-}\mu\text{m}$ -wide microbridges, patterned in epitaxial  $200\text{-nm}$ -thick YBCO films, laser ablated onto MgO substrates. The bridges were placed across  $150\text{-}\mu\text{m}$ -wide, Au-covered, YBCO coplanar transmission lines (CTL), as shown in Fig. 95.39. The test structures were characterized by a zero-resistance transi-

tion temperature  $T_{c0} = 86.8$  K and a transition width  $\Delta T = 0.8$  K. Figure 95.40 presents the family voltage versus current  $V(I)$  characteristics of our microbridge, taken at several temperatures below  $T_c$ . The resistive state with flux-creep behavior, seen as the power-law  $V \sim I^n$  dependence, is clearly visible with no hysteresis upon the current ramping. The inset in Fig. 95.40 shows the  $I_c(T)$  dependence near  $T_c$ . The lower-temperature measurements showed that  $J_c$  was  $> 3$  MA/cm<sup>2</sup> at 77 K.



Z2637

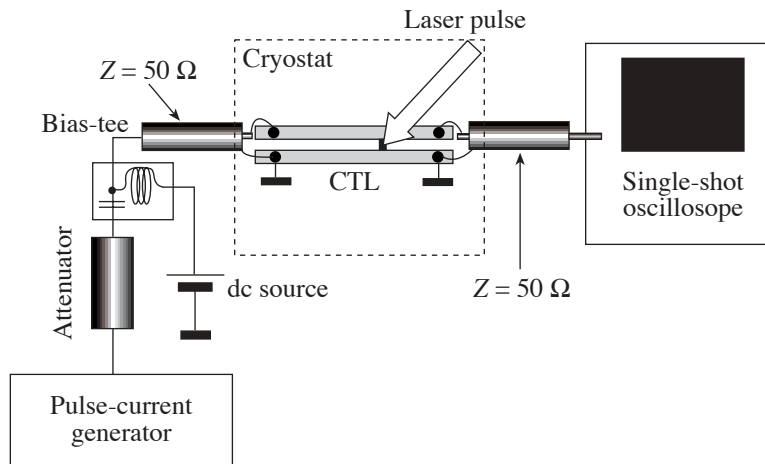


Z2638

Our experimental setup for transient photoresponse measurements of YBCO microbridges biased with supercritical current pulses is shown in Fig. 95.41. The YBCO microbridge was mounted on a cold finger, inside a temperature-controlled, continuous-flow helium cryostat. Nanosecond electrical pulses were delivered from a current generator via a semirigid coaxial cable wire-bonded to the CTL (see also Fig. 95.39). The dc bias was provided from an independent, stable current source and was combined with the pulses via a broadband bias-tee. The

Figure 95.39 Schematic of a 50- $\mu$ m-long, 25- $\mu$ m-wide YBCO microbridge incorporated into the Au-covered YBCO coplanar transmission lines used in our experiments.

Figure 95.40 Voltage versus current characteristics of our YBCO microbridge. The measurement was performed in a two-point configuration, and, subsequently, the constant, temperature-independent resistance of the contacts was numerically subtracted. The inset shows the  $I_c$  dependence on temperature in a region close to  $T_c$ .



Z2639

Figure 95.41 Experimental setup for optical excitation of a superconducting YBCO microbridge, biased with nanosecond-duration current pulses delivered from an electronic pulse generator.

A 3-GHz-bandwidth, single-shot oscilloscope (input impedance of  $50 \Omega$ ) was used to register transient photoresponse signals. The oscilloscope was connected with the sample via a second semirigid coaxial cable wire-bonded to the CTL. The experimental-system time resolution of our recorded transients was approximately 100 ps.

Synchronously with the electrical pulse bias, our superconducting microbridges were illuminated with 100-fs-wide, 810-nm-wavelength optical pulses, picked from an 82-MHz-repetition-rate train of pulses generated by a commercial Ti:sapphire laser. Both the current-pulse generator and the oscilloscope were synchronized with the laser system with the common repetition rate divided down to 32 kHz. The experiments were performed in the temperature range between 80 K and  $T_c$ , with the bulk of the data collected at 80.5 K, where the photoresponse was the largest and the influence of the temperature shift, due to laser heating, was minimized. The temperatures below 80 K were difficult to access since the very large values of  $I_c$  (well over 100 mA) in our samples required the generation of supercritical pulses with amplitudes exceeding the capabilities of our current-pulse generator.

### Experiment Results

An ultrafast voltage transient of the optically excited, current-pulse-biased YBCO microbridge is shown in Fig. 95.42. The bridge was kept at  $T = 80.5$  K and biased with a 10-ns-long current pulse with an amplitude of  $I = 1.1 I_c$ . The main, 10-ns-

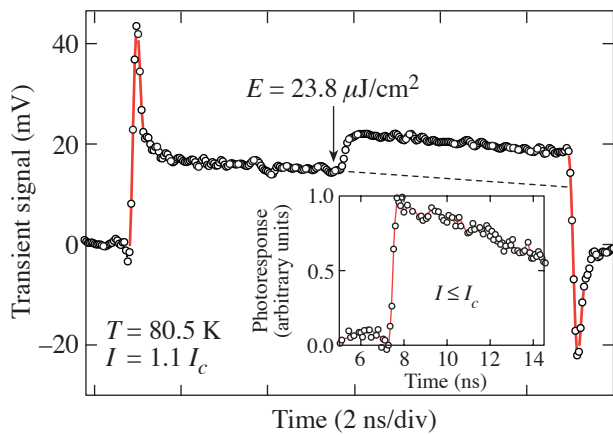


Figure 95.42 Voltage transient generated by a YBCO microbridge, maintained at  $T = 80.5$  K, biased with a 10-ns-long current pulse with amplitude  $I = 1.1 I_c$  and, simultaneously, excited with a 100-fs optical pulse. The arrow shows the arrival of the optical pulse. The inset presents the photoresponse relaxation when the microbridge was biased with the  $I \leq I_c$  current pulse.

long signal, with sharp spikes at the beginning and the end due to the sample inductance, corresponds to the YBCO resistive response to the supercritical current-bias pulse. The arrival of an optical pulse (marked by an arrow in Fig. 95.42) with a fluence of  $23.8 \mu\text{J}/\text{cm}^2$  produced an additional voltage response (photoresponse  $V_{\text{photo}}$ ) with a rise time of less than 100 ps (resolution limit of our experimental setup) and an amplitude of  $\sim 7$  mV. We note that there is apparently no relaxation in the  $V_{\text{photo}}$  transient and the sample remains in the higher-voltage state (see the dashed line indicating the continuation of the electrical transient) until the end of the electrical pulse.

If we assume, for the moment, that the main impact of the light absorption by our YBCO microbridge in the resistive state is just simple heating, we can quickly estimate the magnitude of the heat-generated  $V_{\text{photo}}$ . The incident fluence of  $23.8 \mu\text{J}/\text{cm}^2$  (average power 13.8 mW) should increase the temperature of our bridge by 2.2 K, based on the estimated average temperature increase of 0.16 K/mW, for the 200-nm-thick YBCO uniformly absorbing 810-nm illumination. Analyzing the 80.4-K  $V(I)$  curve shown in Fig. 95.40, the 2.2-K change in temperature should lead to an almost negligible voltage increase across the sample. Since the  $V_{\text{photo}}$  signal in Fig. 95.42 is  $\sim 7$  mV, we can reject the simple-heating model and conclude that the photoresponse must be associated with an optically induced change in the resistive flux state of the microbridge. Photons assist the bias current in the de-pinning of additional vortices in the YBCO film and result in a transition into a higher-voltage state.

The vortex photoresponse model is also consistent with the time evolution of the  $V_{\text{photo}}$  transient. The signal rise time is very short ( $< 100$  ps), indicating an electronic rather than heat-type interaction, and the fact that there is no relaxation after the optical excitation shows that the bridge was optically switched into a new flux state and remained there until the end of the electric pulse, which turned off the resistive state in our microbridge. The latter behavior is very different from the nanosecond-long phonon relaxation observed in the photoresponse of YBCO microbridges current driven into the purely resistive state.<sup>4</sup> In addition, the inset in Fig. 95.42 shows  $V_{\text{photo}}$  for  $I \leq I_c$  (below the edge of the flux-flow state). In this case, the photoresponse is due to the Cooper pair breaking, electron cooling, and the subsequent escape of phonons from the film.<sup>9</sup> As expected, in the inset, the signal relaxes back to the initial level with a decay time of the order of 20 ns—the time scale characteristic for a phonon-escape-type cooling process.

The amplitude of the photoresponse as a function of the normalized current-pulse bias is shown in Fig. 95.43. We note that, initially, the  $V_{\text{photo}}$  amplitude increases very rapidly, reaches the broad maximum value of  $\sim 15$  mV in the  $1.4 < I/I_c < 2.0$  range, and starts to decrease above  $2.0 I_c$ . The above behavior again excludes simple heating; as in the latter case, the resistive/heating contribution would remain constant and result in a linear increase of  $V_{\text{photo}}$  as a function of  $I/I_c$ . On the other hand, in the vortex photoresponse model, the  $V_{\text{photo}}$  signal should depend on the vortex velocity  $v$  of our YBCO microbridge  $v = 2\pi J \rho_n \xi_{a-b}^2 / \Phi_0$ , where  $\rho_n$  is the normal-state (100-K) resistivity of the microbridge,  $\xi_{a-b} = 2.5$  nm (Ref. 10) is the YBCO superconducting coherence length along the  $a$ - $b$  direction,  $\Phi_0 = 2.07 \times 10^{-15}$  Wb is the flux quantum, and  $J$  is the bridge bias current density. Simple calculation shows that for  $\rho_n = 1$  m $\Omega$  cm and  $I = 1.43 I_c$ ,  $v = 2.8 \times 10^4$  cm/s, which is a very reasonable value for current-biased YBCO thin films.<sup>11</sup> For very large  $I/I_c$  values,  $V_{\text{photo}}$  decreases, which must be related to the vortex-velocity decrease associated with vortex-vortex interactions and vortex-antivortex recombination, as well as the reduction of the volume of the superconducting phase. The data presented in Fig. 95.43 allowed us to calculate the voltage responsivity  $R_V$  of our YBCO bridge, defined as the ratio of the  $V_{\text{photo}}$  amplitude to the optical power per pulse incident on the device. The maximal value of  $R_V$ , corresponding to the  $V_{\text{photo}}$  maximum in Fig. 95.43, was found to be  $4.3$   $\mu\text{V}/\text{W}$ .

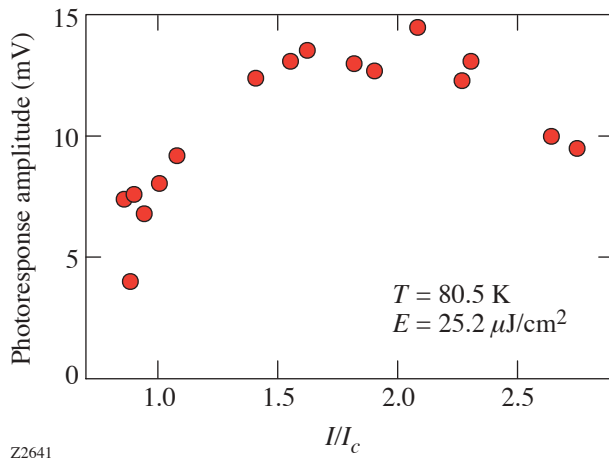


Figure 95.43 The photoresponse amplitude of a YBCO microbridge as a function of the normalized amplitude of the current bias pulse.

Figure 95.44 presents the  $V_{\text{photo}}$  amplitude dependence on the number of photons incident on the microbridge under uniform illumination, for the bias  $I = 1.43 I_c$ . The amplitude increases very rapidly with the laser-fluence increase, reaching a  $13.6$ -mV saturation value at the  $5.9$ - $\mu\text{J}/\text{cm}^2$  fluence. Clearly, this dependence must reflect the process of light-induced generation of vortex-antivortex pairs in our microbridge. The minimal energy  $E_{\text{vp}}$  needed to create a vortex-antivortex pair in a YBCO superconducting film can be expressed as  $E_{\text{vp}} \sim \Phi_0^2 d / (2\pi\mu_0\lambda^2)$ , where  $\mu_0 = 4\pi \times 10^{-7}$  H/m is a permeability of free space,  $\lambda$  is a magnetic penetration depth, and  $d$  is the film thickness. Thus, we have, in our case,  $E_{\text{vp}} \approx 0.65$  eV for  $d = 200$  nm and  $\lambda = 1$   $\mu\text{m}$ .<sup>7</sup> Taking into account that an average radius of single vortex equals  $\xi_{a-b}$ , the maximal number of vortex-antivortex pairs generated in our microbridge is  $\sim 6.4 \times 10^7$ . This latter value corresponds to the onset of saturation of the photoresponse observed in Fig. 95.44; therefore, we can conclude that under our experimental conditions (sample geometry, current bias, etc.) higher laser fluence could not produce additional moving vortices in our YBCO microbridge and the excess light was, apparently, absorbed by the normal phase (free carriers) and converted into joule heating. The high-fluence saturation effect lets us predict that superconducting films with an artificially increased number of pinning centers<sup>8</sup> should exhibit higher amplitudes of  $V_{\text{photo}}$  transients since, in this latter case, the flux-flow state before optical activation would be of lower level due to the increased pinning force.

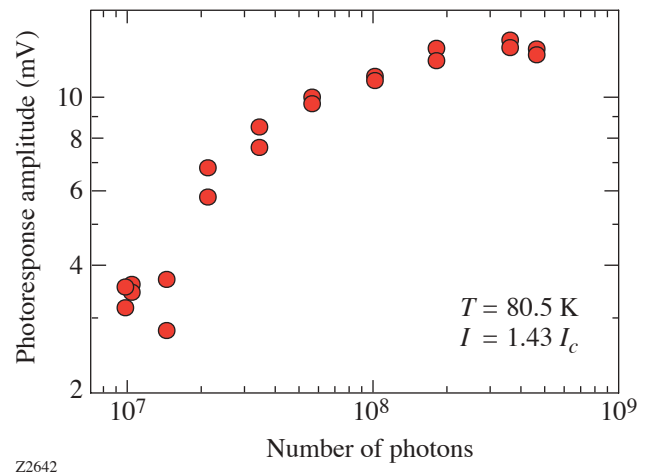


Figure 95.44 The photoresponse amplitude of a YBCO microbridge as a function of the number of photons incident on the structure.

As expected, the photoresponse of the YBCO microbridge was found to be sensitive to the diameter of the laser beam incident on the bridge. Optical imaging experiments have been done at  $T = 80.5$  K with a constant average optical power of 33 mW and a beam diameter ranging from 10  $\mu\text{m}$  to 100  $\mu\text{m}$ . The results shown in Fig. 95.45 demonstrate that the  $V_{\text{photo}}$  amplitude increased with the increase of the spot size, exhibiting a maximum when a whole surface of the YBCO bridge is illuminated. Further opening of the optical beam resulted in a  $V_{\text{photo}}$  decrease since part of the optical energy could not excite the superconductor. The latter behavior is in very good quantitative agreement with the  $V_{\text{photo}}$  dependence on the number of photons incident on the bridge presented in Fig. 95.44.

When the laser beam was focused into a spot with a diameter smaller than the bridge width, photons could create vortices only within the excited hotspot area; the surplus of optical energy was, apparently, dissipated through electron-phonon interaction and diffused as heat toward unilluminated parts of the superconductor. It is worth noting that  $I_c$  variations over the sample length could also account for the  $V_{\text{photo}}$  growth with the hotspot-size growth. This latter line of thought was used to explain small-angle neutron-scattering measurements in Pb-In superconductors with an inhomogeneous surface.<sup>8</sup> It was shown that in the case of superconducting domains possessing different  $I_c$ 's, regions with lower  $I_c$ 's were character-

ized by larger vortex velocities since  $v$  was proportional to  $I - I_c$ . We believe, however, that our films are uniform and, for the fixed current bias,  $v$  is constant, as was discussed in connection with Fig. 95.43.

The maximum repetition rate of the photoresponse generated by our YBCO microbridge can be estimated by progressively reducing the width of the supercritical biasing pulse, while maintaining synchronization of the optical pulse. Figure 95.46 presents the  $V_{\text{photo}}$  signal on top of the 1-ns-wide biasing transient. The minimum width of  $V_{\text{photo}}$  that we could resolve was  $\sim 100$  ps, resulting in the maximum repetition rate in the GHz-frequency range. The main limitation on the maximum repetition rate of the vortex photoresponse signal comes actually not from optical triggering, but from the delay time  $t_d$  of the formation of the resistive state in a superconductor excited by a supercritical current pulse.<sup>12,13</sup> In Ref. 12, for 20-ns-wide supercritical pulses,  $t_d$  was limited by the phonon escape time and was of the order of nanoseconds. For our 1-ns-wide current pulses with a rise time and a fall time of 47 ps and 110 ps, respectively,  $t_d = 210$  ps for  $I \sim I_c$  and decreased down to 140 ps when  $I = 1.5 I_c$ . Clearly, our much faster supercritical perturbations lead to the nonequilibrium state in YBCO;  $t_d$  in this case was limited by  $\sim 1$ -ps electron-phonon interaction time and is predicted to be of the order of hundreds of picoseconds,<sup>14</sup> in agreement with our measurements. Independently, following Ref. 15, one could attribute the very short value of

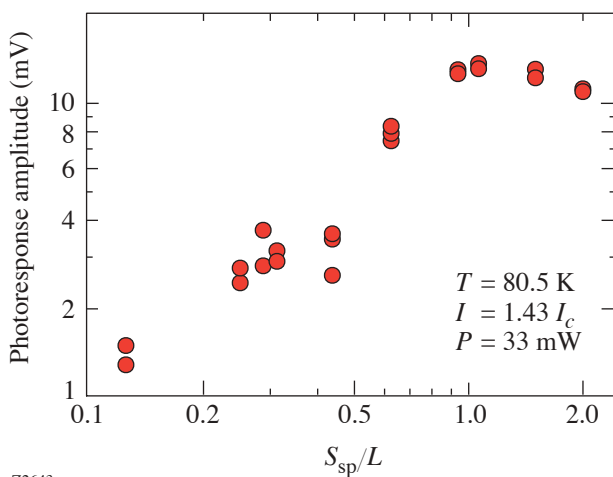


Figure 95.45  
The photoresponse amplitude of a YBCO microbridge as a function of the laser beam diameter, normalized to the microbridge length.

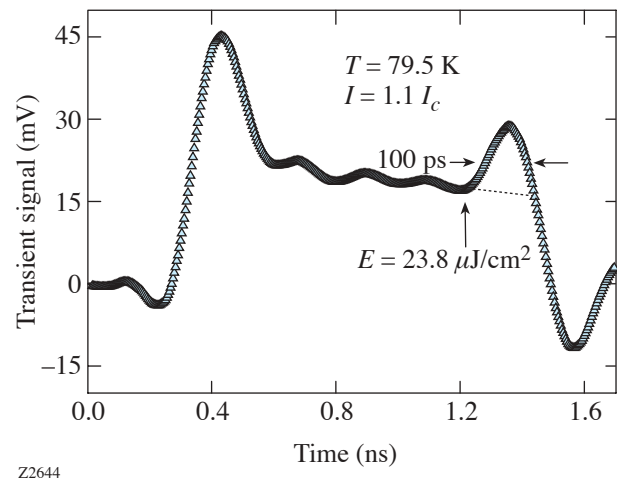


Figure 95.46  
Voltage transient generated by a YBCO microbridge biased with a 1-ns-wide current pulse with amplitude  $I = 1.1 I_c$  and, simultaneously, excited with a 100-fs optical pulse. The arrow shows the arrival of the optical pulse. The photoresponse signal is approximately 100 ps wide.

$t_d$  to the ultrafast magnetic diffusion process when the superconducting bridge is transferred to the flux-flow state. More research is needed to understand the nonequilibrium switching dynamics of YBCO under the picosecond-wide, supercritical current-pulse perturbation, but this subject goes beyond the scope of this article.

### Summary and Conclusions

We have demonstrated the photoresponse effect in YBCO microbridges driven into the resistive flux state by nanosecond-wide supercritical current pulses and synchronously excited with femtosecond optical pulses. It has been shown that the dynamics of the photoresponse is directly related to the motion of vortices in the superconductor. The amplitude of the photoresponse signal can be increased by a factor of 3 when the bias current increases from  $I_c$  to  $1.9 I_c$ , corresponding to the vortex velocity of  $\sim 3 \times 10^4$  cm/s. The photoresponse amplitude also increased with the increase of the laser fluence incident on the device and reached the saturated value when light illuminated the entire microbridge, simultaneously producing the maximal number of vortex-antivortex pairs generated in our microbridge. The above conditions corresponded to the maximal value of the bridge voltage responsivity, which was calculated to be  $\sim 4 \mu\text{V/W}$ . The time-resolved measurements of the vortex photoresponse dynamics showed that signals as short as  $\sim 100$  ps (our experimental resolution limit) could be generated, providing that synchronization with electrical bias pulses was preserved. From the applied point of view, we demonstrated that the YBCO superconductor in the flux-flow state can operate as a GHz-rate, high-power optically triggered switch at supercritical bias current pulses as high as  $2 I_c$ .

### ACKNOWLEDGMENT

The authors thank Grzegorz Jung from the Ben Gurion University for valuable discussions. This work was supported by the National Science Foundation Grant DMR-0073366 and the U.S.–Israel Binational Science Foundation Grant No. 2000164. A. J. acknowledges support from the Fulbright Scholar Program.

### REFERENCES

1. M. J. Lancaster, *Passive Microwave Device Applications of High Temperature Superconductors* (Cambridge University Press, New York, 1997) and references therein.
2. P. E. Goa *et al.*, Appl. Phys. Lett. **82**, 79 (2003).
3. A. Abrutis, J. P. Sénateur, F. Weiss, V. Kubilius, V. Bigelyte, Z. Saltyte, B. Vengalis, and A. Jukna, Supercond. Sci. Technol. **10**, 959 (1997).
4. M. Lindgren, M. Currie, C. Williams, T. Y. Hsiang, P. M. Fauchet, R. Sobolewski, S. H. Moffat, R. A. Hughes, J. S. Preston, and F. A. Hegmann, Appl. Phys. Lett. **74**, 853 (1999).
5. A. Jukna, J. Phys. IV, Proc. **11**, Pr11-151 (2001).
6. A. M. Kadin and M. W. Johnson, Appl. Phys. Lett. **69**, 3938 (1996).
7. A. M. Kadin *et al.*, Appl. Phys. Lett. **57**, 2847 (1990).
8. A. Pautrat *et al.*, Phys. Rev. Lett. **90**, 087002 (2003).
9. See, e.g., A. D. Semenov, G. N. Gol'tsman, and R. Sobolewski, Supercond. Sci. Technol. **15**, R1 (2002).
10. P. P. Nguyen *et al.*, Phys. Rev. B, Condens. Matter **48**, 1148 (1993).
11. S. G. Doettinger *et al.*, Phys. Rev. Lett. **73**, 1691 (1994).
12. G. Sabouret, C. Williams, and R. Sobolewski, Phys. Rev. B, Condens. Matter **66**, 132501 (2002).
13. F. S. Jelila *et al.*, Phys. Rev. Lett. **81**, 1933 (1998).
14. C. Williams, G. Sabouret, and R. Sobolewski, IEICE Trans. Electron. **E85-C**, 733 (2002).
15. Y. S. Cha and T. R. Askew, Physica C **302**, 57 (1998).

